Bull. Nov. Comp. Center, Num. Model. in Atmosph., etc., 5 (1999), 41–53

On sensitivity of the World Ocean model to the vertical resolution

A.V. Scherbakov, V.V. Malakhova

The three-dimensional linear model of the World ocean climate (with real bottom) is presented. The numerical method is based on the implicit schemes. The equations of heat and salt transport with respect to horizontal coordinates are approximated by the nine-point difference scheme, obtained by the Richardson extrapolation. The second up-wind scheme is used in the vertical coordinate. A series of numerical experiments was carried out till the steady states for 12, 24, 36 vertical levels. The global distribution of temperature and salinity fields is in agreement with observations, though the model does not simulate the Antarctic Intermediate Water and deep water too fresh. After five thousand years of integration, the stationary solution contains oscillations with different periods varying from a few years to hundreds. The influence of the vertical resolution on the average temperature of the ocean is analyzed.

1. Introduction

The World Ocean is one of the most important components of the climate system.

On time scales from weeks to thousands of years, the dynamics of climate is strongly controlled by the behavior of the oceans since the ocean circulation moves large amounts of heat around the planet. Recently, it has been established that the hypothesis about a slow ocean variability appears to be wrong, [1]. The sensitivity of the large-scale general circulation to thermohaline forcing was shown by Maier-Reimer et al. [2]. The main reason of this sensitivity is the formation of deep water at high latitudes, which strongly depends on the heat exchange with the atmosphere. If the deep cold water is formed, this means that the average temperature must be about 3.6°C, [3].

In previous works [4, 5], a series of numerical experiments with a three-dimensional numerical model of the global ocean climate with a flat bottom were described. The temperature of the deep ocean has appeared higher than it should be. In this work, the global circulation model of the World Ocean including seasonal changes of temperature, salinity and wind stress at the see surface, bottom topography is represented.

Due to simplicity of the present numerical model of the ocean, it appeared possible to increase the time of integration of the model till 5000

years and even higher and to detect basic features of the large-scale circulation and climatic state of the World Ocean at different resolutions with respect to the vertical coordinate. The average temperature of the ocean was 4.2–3.8°C in accordance with the vertical resolution.

The stationary solution contains the same oscillations as in [6–8]. In these experiments, variations with periods from 3 to 20 years are most significant.

2. Numerical model of the ocean thermohaline circulation

Let us consider the problem of formation of the large-scale climatic temperature, salinity and currents fields in the World Ocean including the Arctic ocean with real geometry and bottom topography. Consider the basic system of equations, where the hydrostatic, Boussinesq's and rigid lid approximation are employed, and nonlinear terms in the equations of motion are omitted, [4]:

$$R_1 u + \ell v = -\frac{1}{a\rho_0 \sin\theta}\frac{\partial P}{\partial \lambda} + \frac{\partial}{\partial z}\nu\frac{\partial u}{\partial z}, \tag{1}$$

$$-\ell u + R_1 v = -\frac{1}{a\rho_0}\frac{\partial P}{\partial \theta} + \frac{\partial}{\partial z}\nu\frac{\partial v}{\partial z}, \tag{2}$$

$$\frac{1}{a\sin\theta}\left(\frac{\partial u}{\partial \lambda} + \frac{\partial v \sin\theta}{\partial \theta}\right) + \frac{\partial w}{\partial z} = 0, \tag{3}$$

$$P = -g\rho_0\zeta + g\int_0^z \rho\, dz, \tag{4}$$

$$\frac{\partial \Phi}{\partial t} + \frac{u}{a\sin\theta}\frac{\partial \Phi}{\partial \lambda} + \frac{v}{a}\frac{\partial \Phi}{\partial \theta} + w\frac{\partial \Phi}{\partial z} = \frac{\partial}{\partial z}æ\frac{\partial \Phi}{\partial z} + \frac{\mu}{a^2}\Delta\Phi, \tag{5}$$

where

$$\Delta\Phi = \frac{1}{\sin^2\theta}\frac{\partial^2\Phi}{\partial\lambda^2} + \frac{1}{\sin\theta}\frac{\partial}{\partial\theta}\sin\theta\frac{\partial\Phi}{\partial\theta}, \quad \Phi = (T, S);$$

$$\rho = \rho_0 + 10^{-3}[0.802(S-35) - T(0.0735 + 0.00469T)]. \tag{6}$$

The boundary conditions for $z = 0$:

$$\nu\frac{\partial u}{\partial z} = -\frac{\tau_\lambda}{\rho_0}, \quad \nu\frac{\partial v}{\partial z} = -\frac{\tau_\theta}{\rho_0}, \quad w = 0, \quad T = T^*(t,\lambda,\theta), \quad S = S^*(t,\lambda,\theta). \tag{7}$$

The boundary conditions for $z = H$:

$$\nu\frac{\partial u}{\partial z} = -R_2\int_0^H u\, dz, \quad \nu\frac{\partial v}{\partial z} = -R_2\int_0^H v\, dz,$$

$$w(H) = \frac{u(H)}{a\sin\theta}\frac{\partial H}{\partial\lambda} + v(H)\frac{\partial H}{\partial\theta}, \quad æ\frac{\partial T}{\partial z} = 0, \quad æ\frac{\partial S}{\partial z} = 0; \tag{8}$$

at the lateral wall Γ:

$$\mu\frac{\partial T}{\partial n}=0,\quad \mu\frac{\partial S}{\partial n}=0,\quad u_n=0, \tag{9}$$

at the initial moment $t=0$:

$$T=\tilde{T}(z),\quad S=\tilde{S}(z). \tag{10}$$

The equations are presented in the spherical coordinate system (λ is latitude, θ is the addition of longitude up to 90°, the axis z is directed vertically downwards); u, v, w are velocity vector components, t is time, ρ_0, ρ are the mean value and the anomaly of density respectively, $\zeta = \xi - P_{\text{atm}}/(g\rho_0)$ is the reduced level, P_{atm} is the atmospheric pressure, $z = \xi(\lambda,\theta)$ is the equation of the ocean surface, $R_1 u$, $R_1 v$ is the parameterization of the horizontal turbulent viscosity, ν is the vertical turbulent viscosity coefficient, æ, μ are the vertical and horizontal turbulent temperature and salinity diffusion coefficients, $\ell = 2\omega\cos\theta$ is the Coriolis parameter, a, ω, and g are the radius, the angular velocity, and acceleration of gravity of the Earth, respectively, τ_λ, τ_θ is the wind stress, T^*, S^* are the known climatic distributions of temperature and salinity at the ocean surface, R_2 is the bottom friction coefficient, n is the normal to the lateral cylindrical wall Γ, H is the bottom topography.

The method of solving problem (1)–(10) is described in detail in [4], here we only mention that for equation (5), on the uniform five-degree grid, the horizontal operator is approximated by the nine-point difference scheme, obtained by the Richardson extrapolation, [9], and the vertical operator, after introduction of a new variable, condensing the grid at the ocean surface, is approximated by the second up-wind scheme, [10].

The uniform five-degree grid is shifted by 2.5° relative to the equator, and the lateral boundary Γ is inserted in the polygonal area approximating the World Ocean from 72.5° S to 87.5° N. The model includes a realistic smoothed bottom topography. Two grids condensing near the ocean surface from the square law are introduced into the vertical coordinate. On one grid with the integer-valued meanings of the index k:

$$z_k=(\eta_N-\eta_0)^2[(k-1/2)/N]^2, \tag{11}$$

where $\eta_N^2 = H+\alpha$, $\alpha = 120$ cm, the variables u, v, T, S, ρ are defined. The points of the second grid are in the middle of the intervals

$$z_{k+1/2}=\frac{z_{k+1}+z_k}{2},\quad z_{1/2}=0,\quad z_{N+1/2}=H, \tag{12}$$

where N is the number of vertical levels.

3. The numerical experiments

Three experiments were carried out with this model: R12 – with 12 levels in the vertical, R24 – with 24 levels and R36 with 36 levels.

In all the experiments, the horizontal diffusion coefficients $\mu_\lambda = \mu_\theta = 3.6 \cdot 10^7$ everywhere, except for the equator belt of 3 grid steps wide and with a depth less than 500 m, where μ_λ was increased to $3.6 \cdot 10^9$. The value of the coefficient R_1 near the equator is multiplied by 10^3. Other parameters used in the numerical experiment are the following (in CGS):

$$R_1 = 4.5 \cdot 10^{-6}, \quad R_2 = 0.5 \cdot 10^{-7}, \quad \nu = 75, \quad æ = 0.2,$$
$$a = 6.4 \cdot 10^8, \quad \omega = 0.73 \cdot 10^{-4}, \quad \rho_0 = 1.02541, \quad g = 980.$$

In all the experiments, the global ocean model was forced by the seasonally varying climatic temperature, salinity, [3], and wind stress at the ocean surface. In each experiment, the model was run with the time step of 10 days for 5000 years until equilibrium. Figure 1 shows time series of the global winter average temperature during these 5000 years for all the experiments.

In experiment R12, the average temperature of the ocean was 4.24°C, with the increase of the vertical resolution up to 24 levels, in the next experiment R24 it has decreased to 3.93°C, and in experiment R36 – to 3.78°C. It

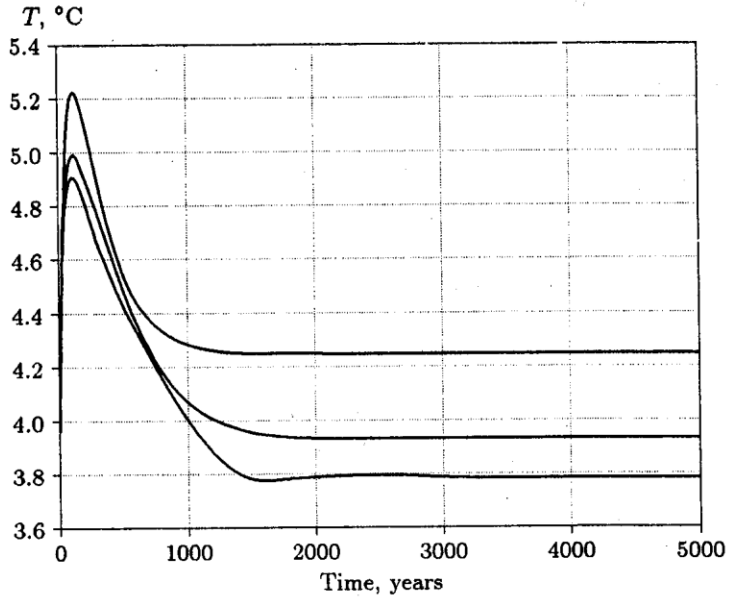

Figure 1. Time series for the average winter temperature for 5000 years in R12 – the upper, R24 – the middle, and R36 – the lower line

is known, that the average temperature of the ocean according to observations data is equal to 3.62°C, [3], however, if we calculate this value using the observed temperature data on 12 standard levels, the average temperature will appear equal to 4.1°C.

Figures 2, 3, 4 show the profiles of the globally averaged temperature, salinity and density for all the experiments for the winter season, together with the winter values from Levitus, [3]. The effect of increasing the vertical resolution is clearly apparent in the more real water mass simulation. The thermocline, the halocline and the pycnocline structures are improved with a high resolution, the numerical solution tending to the observed profiles. The increase of the space resolution in the vertical has decreased the deep ocean temperature, and its values are compared to the observed data. However, the saline simulation is poor in all the cases. The marked salinity minimum at a depth of about 800–1000 m is completely absent, and the deep water is too fresh.

If in the previous experiments with the flat bottom [4, 5], the temperature of nearbottom waters of the ocean in the tropical and the subtropical latitudes was about 3–3.5°C, now these values are between 1–2.5°C in experiment R12, 0.5–1.5°C in R24 and 0–1.5°C in R36. This means that the model has reproduced the cold bottom water. The deep water formation is found in the North Atlantic and the South oceans.

It should be noted that the effect of a reduced $æ$ from 1 in [4, 5] till 0.2 leads to the real average and deep water temperature.

The globally averaged latitude-depth sections of temperature and salinity in experiments R12, R24, R36 are shown in Figures 5, 6 and 7. In all three experiments, both temperature and salinity fields are in agreement with observations and remain essentially the same. There is a qualitatively realistic thermocline, which is shallow near the equator and deep in the subtropical latitudes. The saline structure seems to be not so good as the temperature one. Except the main halocline, the deep salinity structure does not bear the qualitative resemblance to that by Levitus, [3]. There is not any northward penetration of fresh Antarctic intermediate water, and the simulated deep and bottom water is too fresh.

In all the experiments, the deep water formed in the Southern Ocean sinks to the bottom rather than to intermediate levels. Figures 5–7 show the beginning of the formation of the highly saline cold deep water of the World Ocean, when the highly saline cold North Atlantic water sinks into the deeper layers but does not spread near the bottom towards the Southern hemisphere. It should be noted that in the deep ocean, the water is 0.25–0.15 psu fresher than that observed, i.e., 34.45–34.55 psu instead of 34.7 psu, [3]. Perhaps it is connected with the rough horizontal resolution of the model and the absence of parameterization of the saline Mediterranean and the Red sea water.

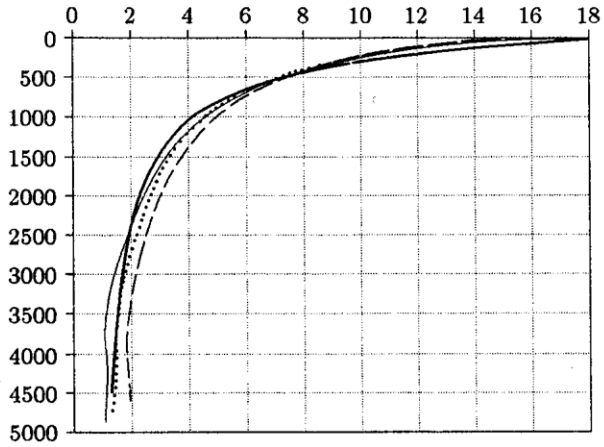

Figure 2. Vertical profiles of temperature from R12 (long dashes), from R24 (short dashes), from R36 (thin line) and from Levitus' climatology (thick line)

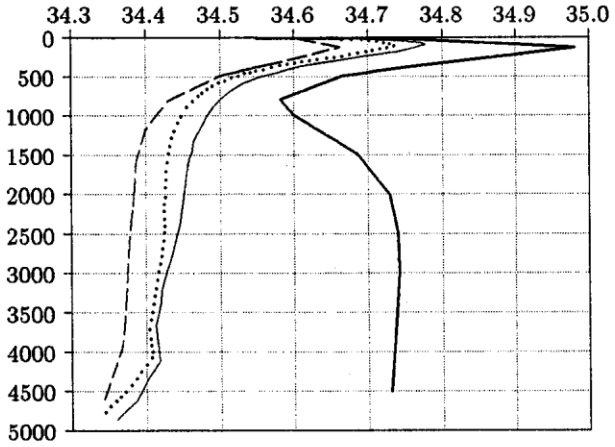

Figure 3. Vertical profiles of salinity from R12 (long dashes), from R24 (short dashes), from R36 (thin line) and from Levitus' climatology (thick line)

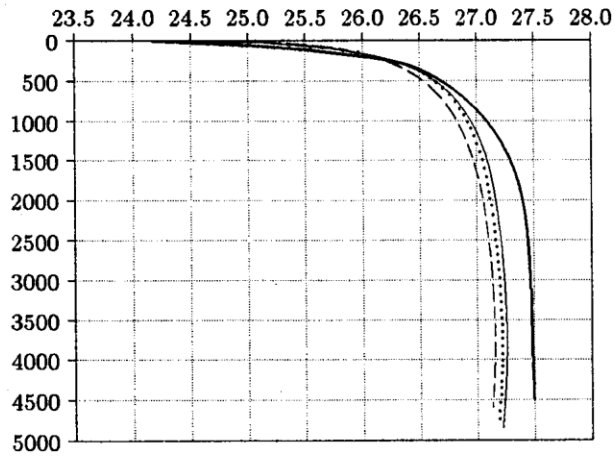

Figure 4. Vertical profiles of density from R12 (long dashes), from R24 (short dashes), from R36 (thin line) and from climatology of Levitus (thick line)

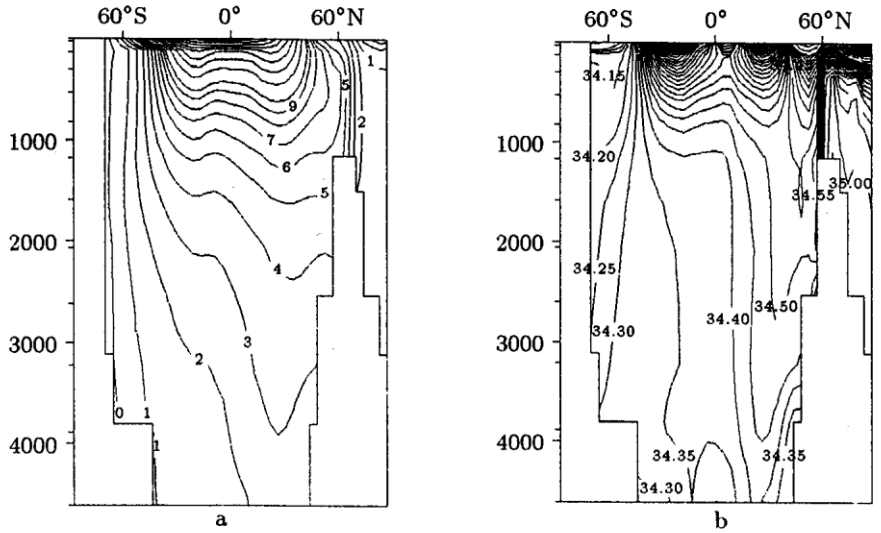

Figure 5. Zonally averaged temperature in °C (a) and salinity in psu (b) of the global ocean from R12

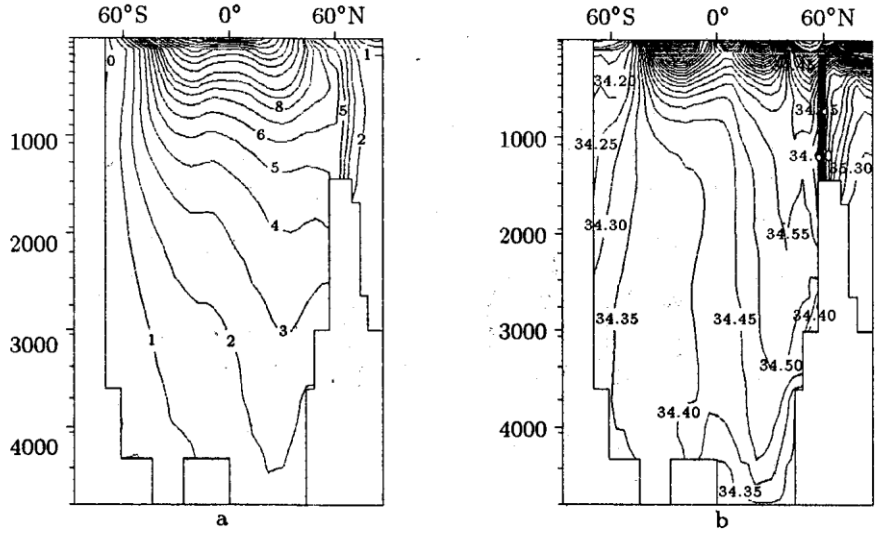

Figure 6. Zonally averaged temperature in °C (a) and salinity in psu (b) of the global ocean from R24

A more detailed examination of the time series of the global average temperature shows that there exist persistent oscillations with different periods. We continued experiment R36 till 20000 years. The average temperature continues to change in 4–5 decimal positions after a comma, as one can see from Figure 8, where the last 14000 years for R36 are shown. The period

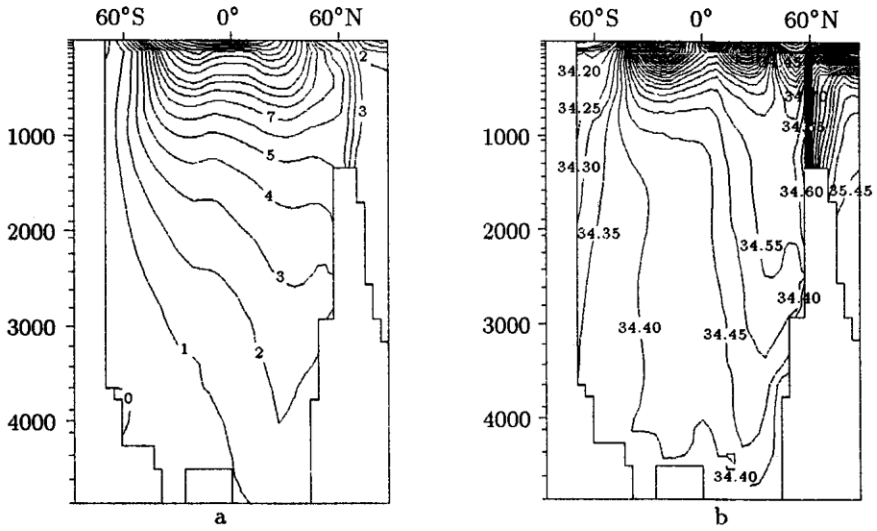

Figure 7. Zonally averaged temperature in °C (a) and salinity in psu (b) of the global ocean from R36

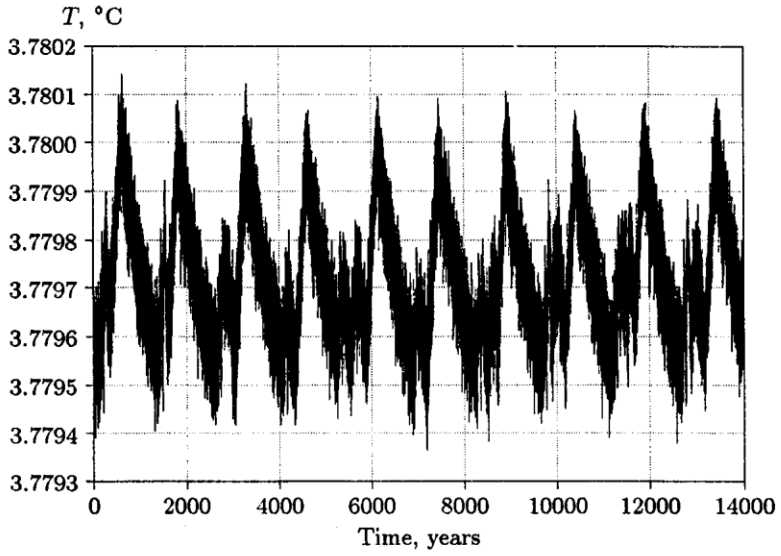

Figure 8. Time series for the average winter temperature for the last 14000 years in R36

of oscillations depends on the vertical resolution of the model. So, in R12, the periods of 2.5, 9–12, 20, and 600 years are most prominent, in R24, 3 and 12 years, and in R36, 2, 10–12, 36, and 1200–1600 years. In the paper by Zalesny [6], in similar experiments with a global ocean model with 11 vertical levels, the oscillations in 3–4 decimal positions with the periods of

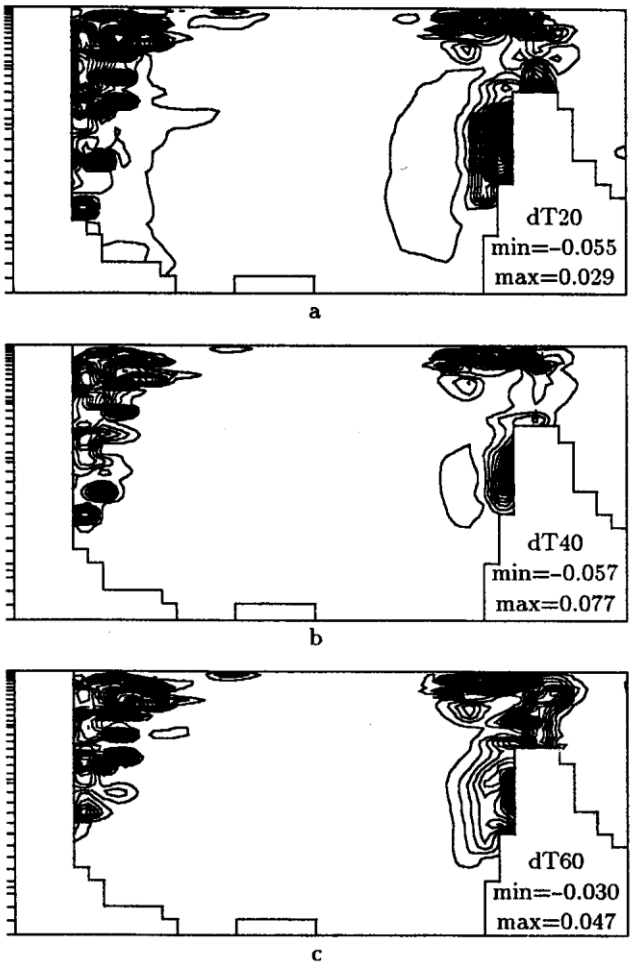

Figure 9. Zonally averaged anomaly of the temperature after 20 (a), 40 (b), and 60 (c) years

3 and 10 years are also obtained. In [7], the most pronounced self-sustained oscillations with a time scale of 20, 360, and 1100 years are obtained. In our previous work, in the model with a flat bottom and zero wind, [5], oscillations with periods 2.3 and 1150 years were found.

To investigate the reason of these oscillations, we average the temperature field over 1600 years and compute the temperature anomaly after various time intervals. The zonally average temperature anomalies after 20, 40, and 60 years are shown in Figure 9. One can see that all the anomalies are in the regions of the deep water formation, where the deep convection takes place.

Figures 10 and 11 show the space distribution of the places of these oscillations. It is the regions of strong advective transport, such as GolfStream,

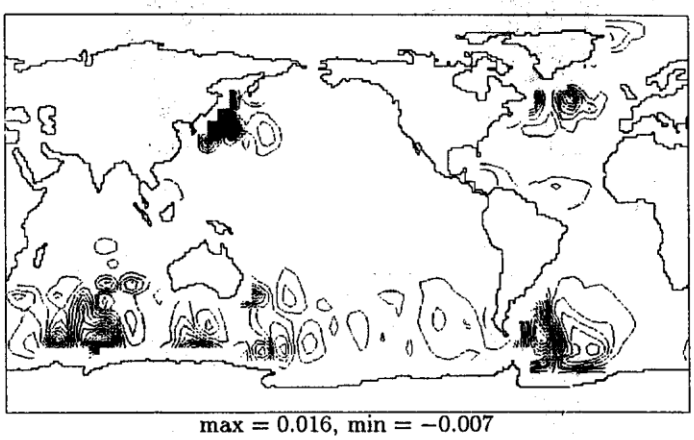

max = 0.016, min = −0.007

a

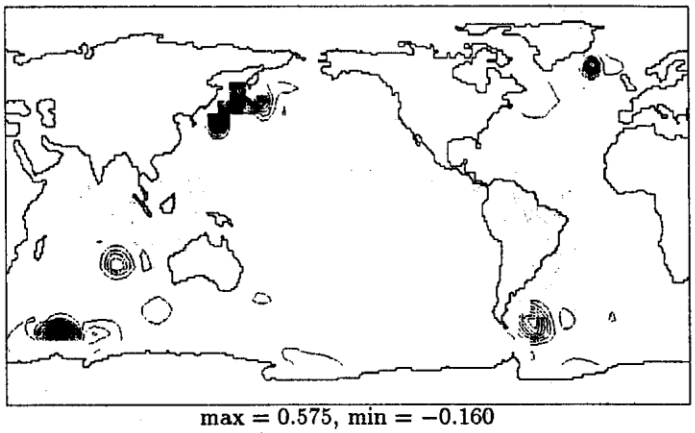

max = 0.575, min = −0.160

b

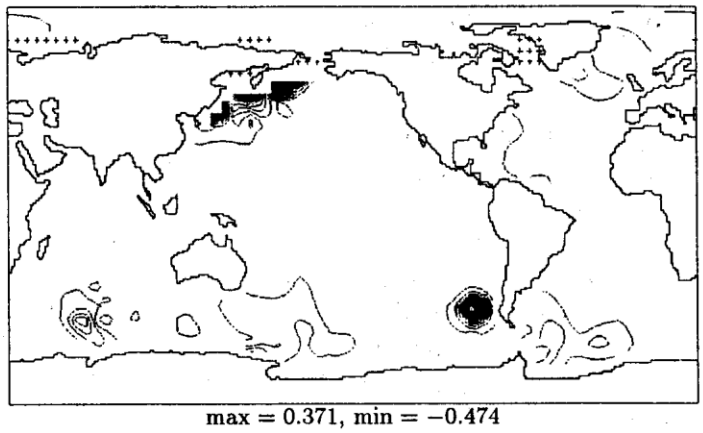

max = 0.371, min = −0.474

c

Figure 10. The temperature anomaly after 20 years at 7.7 m (a), 90.7 m (b), and 298.7 m (c)

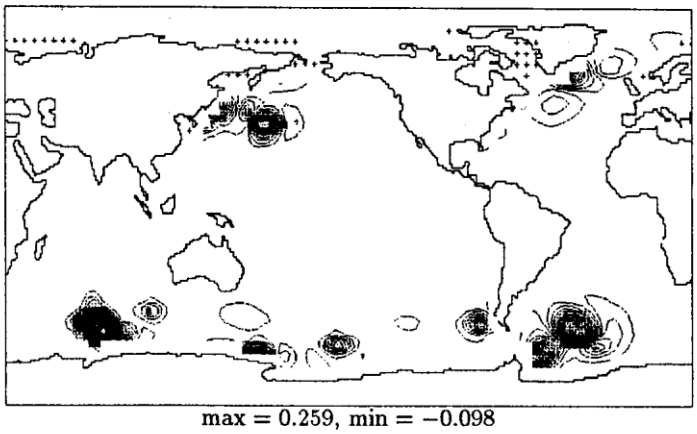

max = 0.259, min = −0.098

a

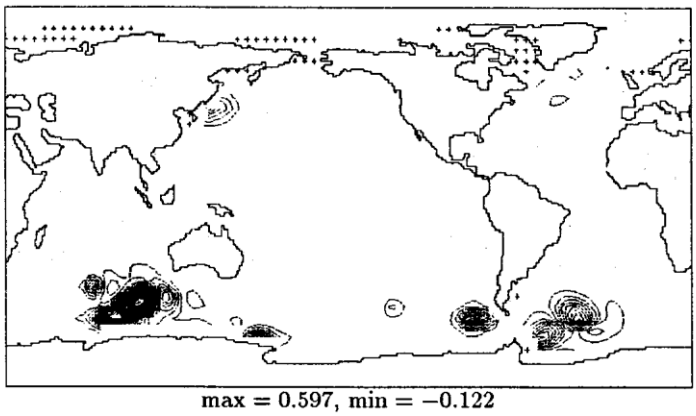

max = 0.597, min = −0.122

b

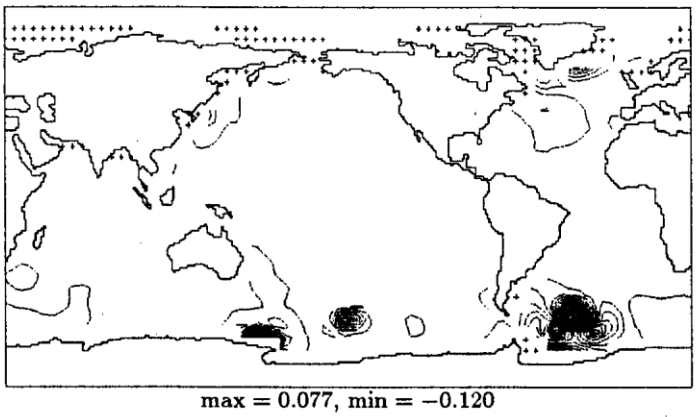

max = 0.077, min = −0.120

c

Figure 11. The temperature anomaly after 20 years at 444.4 m (a), 617.8 m (b), and 1048.3 m (c)

Kurosio, the Antarctic Circumpolar Current near Ross and the Weddell Sea and the south part of the Indian ocean, which contain such oscillations.

Analysis of the horizontal structure of these oscillations in the temperature field has shown, that in definite places of the World Ocean with a strict periodicity in some years, the oscillations with amplitude up to 0.1–0.4 degrees are present. For example, periodic oscillations with an amplitude of 0.28°C at a depth of 528 m in the area of Kurosio, with an amplitude of 0.3, 0.32, and 0.39°C at depths of 299, 819, and 1590 m between the Antarctic Continent and Australia.

4. Conclusions

The principal conclusions of this work may be summarized as follows:

1. The increase of the vertical resolution in the large-scale geostrophic model with a bottom topography results in a better reprodution of the global ocean temperature and salinity fields. The model predicts the realistic thermocline and halocline, it reproduces the real deep water temperature and the average global temperature. The model is not capable to reproduce the complex vertical salinity structure in the Southren hemisphere.

2. Time series of the winter global average temperature under the equilibrium state contain oscillations with an amplitude of 10^{-4}–10^{-5} degrees and the periods of approximately from 3 to 10 years till 1600 years.

References

[1] Zavarzin G.A., Kotliakov V.M. The strategy of study The Earth in light of global modifications // Bulletin of RAS. – 1998. – Vol. 68, № 1. – P. 23–29 (in Russian).

[2] Maier-Reimer E., Mikolajewicz U., Hasselmann K. Mean circulation of the Hamburg LSG OGCM and sensitivity to the thermohaline surface forcing // J. Phys. Oceanogr. – 1995. – Vol. 23. – P. 731–757.

[3] Levitus S. Climatological Atlas of the World Ocean / NOAA Prof. Paper, 13. – U.S. Govt. Printing Office, 1982.

[4] Scherbakov A.V., Malakhova V.V., Antsis E.N. Numerical model of the World Ocean with the Arctic ocean taken into account. – Novosibirsk, 1997. – (Preprint / RAN. Siberian Branch. Inst. of Comp. Math. and Math. Geoph.; 1106) (in Russian).

[5] Scherbakov A.V., Malakhova V.V., Nepomnjaschy V.G. About receiving stationary solutions of the linearized problem of the World Ocean climate. – Novosibirsk, 1998. – (Preprint / RAN. Siberian Branch. Inst. of Comp. Math. and Math. Geoph.; 1141) (in Russian).

[6] Zalesny V.B. Numerical simulation of the thermohaline circulation of World Ocean // Meteorology and hydrology. – 1998. – № 2. – P. 54–67 (in Russian).

[7] Drijhout S., Heinze C., Latif M., Maier-Reimer E. Mean circulation and internal variability in a ocean primitive equation model // J. Phys. Oceanogr. – 1996. – Vol. 26, № 4. – P. 559–580.

[8] Zalesny V.B., Moshonkin S.N. Equilibrium thermohaline regime of model global ocean circulation // Izvestia RAN FAO. – 1999. – Vol. 35, № 3. – P. 371–398 (in Russian).

[9] Scherbakov A.V., Moiseev V.M. The difference scheme for the advective-diffusion equation. – Novosibirsk, 1985. – (Preprint / RAN. Siberian Branch. Computing Center; 631) (in Russian).

[10] Roache P.J. Computational Fluid Dynamics. – Albuqerque: Hermosa Publishers, 1976.

[11] Moore A.M., Reason C.J. The response of a global ocean general circulation model to climatological surface boundary conditions for temperature and salinity // J. Phys. Oceanogr. – 1993. – Vol. 23. – P. 300–328.